applied sciences

MDPI

Article

Adsorption of Chromium (VI) on Calcium Phosphate: Mechanisms and Stability Constants of Surface Complexes

Ahmed Elyahyaoui [1,*], Kawtar Ellouzi [1], Hamzeh Al Zabadi [2], Brahim Razzouki [3], Saidati Bouhlassa [1], Khalil Azzaoui [4], El Miloud Mejdoubi [4], Othman Hamed [5], Shehdeh Jodeh [5,*] and Abdellatif Lamhamdi [4,6]

1 Laboratory of Radiochemistry, Department of Chemistry, Faculty of Sciences, Mohamed V-Agdal, B.P 1014 Rabat, Morocco; ellouzi.kawtar@gmail.com (K.E.); bouhlass@fsr.ac.ma (S.B.)
2 Public Health Department, An-Najah National University, P.O. Box 7, Nablus 44830, Palestine; halzabadi@gmail.com
3 Laboratory of Spectroscopy, Molecular Modeling, Materials and Environment, Department of Chemistry, Faculty of Sciences, Mohamed V, B.P 1014 Rabat, Morocco; bramrwk@gmail.com
4 Laboratory LMSAC, Faculty of Sciences, Mohamed 1st University, P.O. Box 717, Oujda 60000, Morocco; k.azzaoui@yahoo.com (K.A.); ee.mejdoubi@gmail.com (E.M.M.); abdellatiflamhamdi@hotmail.com (A.L.)
5 Department of Chemistry, An-Najah National University, P.O. Box 7, Nablus 44830, Palestine; ohamed@najah.edu
6 National School of Applied Sciences Al Hoceima, Mohamed 1st University, P.O. Box 717, Oujda 60000, Morocco
* Correspondence: yahyaoui@fsr.ac.ma (A.E.); sjodeh@hotmail.com (S.J.); Tel.: +212-537-77-54-40 (A.E.); +970-599-590-498 or +970-923-459-82 (S.J.)

Academic Editor: Faisal Ibney Hai
Received: 4 December 2016; Accepted: 7 February 2017; Published: 28 February 2017

Abstract: The adsorption of chromate on octacalcium phosphate (OCP) was investigated as a function of contact time, surface coverage, and solution pH. The ion exchange method was adapted to establish the interaction mechanism. Stoichiometry exchange of H^+/OH^- was evaluated at a pH range of 3–10, and obtained values ranged between 0.0 and 1.0. The surface complexes formed between chromate and OCP were found to be $\overline{> S(HCrO_4)}$ and $\overline{> S(CrO_4)}$. The logarithmic stability constant $logK_{1\text{-}1}$, and the $logK_{10}$ values of the complexes, were 6.0 in acidic medium and 0.1 in alkaline medium, respectively. At low pH and low surface coverage, the bidentate species $\overline{> S(HCrO_4)_2}$ with $logK_{10.5}$ of about 2.9, was favored at a hydration time of less than 150 min. The contribution of an electrostatic effect to the chromium uptake by the OCP sorbent, was also evaluated. The results indicate that the adsorption of chromate on OCP is of an electrostatic nature at a pH $\leq$ 5.6, and of a chemical nature at a pH > 5.6.

Keywords: octacalcium phosphate; chromium (VI); adsorption; environmental; ion exchange

1. Introduction

The hexavalent chromium Cr (VI) generated from various industrial processes, such as metallurgy, dyes, paints, inks, and plastics, is a major global concern, due to its harmful effects on humans and nature [1].

As a result, the presence of this metal cation in nature is well controlled. The maximal concentration level of Cr (VI) allowed in drinking water, as determined by the US-Environmental Protection Agency (EPA), is 0.05 mg/L [2]. Compliance with the EPA's chromium rule requires additional industrial monitoring. Designing a treatment process which reduces the number of

chromium ions in industrial effluent to an acceptable level, has become crucial. A number of methods for this purpose have already been developed, among which are reduction and precipitation [3], ion exchange [4], solvent extraction [5], adsorption [6], and electrochemical precipitation [7]. When considering these methods, adsorption is the most promising technique [8]. This process is usually performed using conventional adsorbents, such as silica, zeolites, iron(III) (hydr)oxides, and activated carbon, or nonconventional adsorbents, such as red mud, sewage sludge, and bone char [9–11]. Phosphate materials (synthetics and minerals) have also been used as effective adsorbents for heavy metals from wastewaters and polluted soils. They have an excellent stabilization efficiency for several metal ions. For this reason, they are highly efficient metal adsorbents [12–14], particularly calcium phosphate. This material has a large specific area, high thermal and geochemical stability, low solubility, high ionic exchange capacity, and high stability towards ionization by radiation. For these reasons, it has been used as a backfill material for geological repositories for nuclear waste [15], and as an adsorbent in engineered barriers for environmental restoration [16]. It was also reported that phosphates with an amorphous structure are more efficient adsorbents of lead, uranium, and plutonium [17].

Although several adsorbents have been developed, and the retention of the metals hasbeen extensively studied, the sorption mechanisms are still rather difficult to identify. This could be because several phenomena, such as iso-morphous substitutions, surface complexation, and dissolution–precipitation, can occur simultaneously during the sorption process [18–21]. In addition, there is a lack of data on the adsorption of many metals on amorphous or poorly-crystallized phosphates.

Published studies show that the uptake of hexavalent chromium by calcium phosphate, exhibits typical anionic (such as $HCrO_4^-$ and CrO_4^{2-}) sorption behavior, and that the adsorption decreases by increasing the pH [22]. They also show that Cr (VI) adsorption is favored on phosphate that ispositively charged, at a low to neutral pH level (i.e., high point of zero charge (PZC)) [23]. The findings suggest that the retention of Cr (VI) by phosphates occurs through an electrostatic attraction and via binding to the surface functional groups OH_2^+ and OH^-. In other studies, it was found that hydroxapatite (HAp) and tricalcium phosphate (TCP) composite are able to adsorb a significant amount of chromium (VI), at a pH level of about 5. So, the composites showed a lower PZC than HAp (6.2–8.5) [22–24].

Moreover, there is no systematic understanding of the mechanism of chromium immobilization that involves the protonation/deprotonation of surface hydroxyl groups, and their interaction with the metal oxyanion. The combined effect of both pH and contact time on the adsorption mechanism requires more investigation (Figure 1).

Taking these considerations into account, the present study aims to investigate the complexation of hexavalent chromium with low-crystallized octacalcium phosphate (OCP). To achieve the aim of this study, the removal of Cr (VI) from aqueous solution was studied through batch experiments, as a function of contact time, the amount of adsorbent, and the equilibrium pH of chromate (10^{-4} M) solution. The ion exchange method, which has already been successfully implemented, especially in solvent extraction, has been chosen by the authors, in order to study the behavior of chromium (VI) on the surface of OCP. Another aim of this work is to investigate the surface complexation of OCP.

2. Experiment

2.1. Materials and Methods

Octacalcium phosphate (OCP) was synthesized in our laboratory. Phosphoric acid (99%), Chromium (VI), Calcium hydroxide (99%), Potassium hydroxide (KOH) (99%), and Nitric acid (HNO_3) (99%), were purchased from Sigma Aldrich, and were used in the same form as they were received. High-purity distilled water was used for all of the experiments.

2.2. Synthesis and Characterization of OCP

Calcium phosphate was synthesized using the microwave-hydrothermal method. In this method, phosphoric acid (0.3 M) and calcium hydroxide solution (0.5 M) are used as the starting materials. The preparation method has been described in [22]. The obtained mixture was heated at 150 °C for 1 h, and then irradiated in a microwave oven (800 w) for 5 min. The resulting gel was filtered off and dried overnight in an air oven, at 80 °C. The obtained solid was repeatedly washed with hot distilled water, and was identified as OCP by the associated XRD patterns and FT-IR. The characteristics of the diffraction line observed in the XRD patterns at $2\theta = 4.7°$, is evidence for the formation of OCP [22].

This result was confirmed by the FTIR characteristic peaks of OCP at 1089 and 1033, and by the Ca/P ratio of 1.34, which was close to the theoretical OCP ratio of 1.33 [25,26].

2.3. Surface Properties and Adsorption Experiments

The adsorption experiments were carried out by a batch method. A stock solution of Cr (VI) (10^{-4} M) was prepared from potassium dichromate. The pH level of the solution was measured using a Hanna combined electrode (Hanna pH 210). Nitric acid and KOH were used to adjust the starting acidity of the aqueous solutions of Cr (VI), with a concentration of 10^{-4} M in all cases. Sorption experiments were conducted at room temperature, as a function of the pH, contact time, and amount of adsorbent (m). The supernatants (5.0 mL) were filtered and analyzed for aqueous chromium using the 1,5-diphenylcarbazide (EPA 7196A) spectrophotometry method. The adsorbed chromium was calculated from the difference between the concentrations before and after equilibrium with calcium phosphate. The ratio of Cr (VI) concentrations in solid and aqueous phases led to the distribution coefficient D.

3. Results and Discussion

3.1. Effect of pH on Chromium Adsorption

The logarithmic variation of D with pH at different contact times, for 0.5, 1.0, and 1.5 g/L of calcium phosphate solutions, is plotted in Figure 1.

As shown in Figure 1, all cases exhibit similar behavior; log D increased by increasing the pH, to reach the maximum at pH_{max} of 4.0 to 5.0, before decreasing as the pH continued to increase. The maximum adsorption efficiencies were found to increase with the amount of adsorbent (m). The results also show that the pH_{max} is dependent on the contact time; when the contact time increased from 5 to 150 min, the pH_{max} rose from about 4 to 5.

The variation in the extraction efficiency with the solution's pH could be related to the protonation/deprotonating of both surface groups, and to the acidity of H_2CrO_4 (pK_{a1} = 0.2 and pK_{a2} = 6.5) [27–29]. According to the chromium speciation pH-diagram, the chromium (VI) was adsorbed as hydrogen chromate ($HCrO_4^-$) at pH $\leq$ 5.0 ($\geq$95%), as chromate (CrO_4^{2-}) at pH $\geq$ 7.6 ($\geq$95%), and as a mixture of these species between pH 5.0 and 7.6. In this case, both electrostatic and chemical sorption mechanisms could occur, and generally, it is not possible to distinguish between these two mechanisms [30]. It was assumed that the maximum adsorption occurred when the combination of a high positive surface charge and a high concentration of anionic chromium species, are achieved. Thus, the uptake of weak acid was maximal at a pH value around its dissociation constant, or near the PZC of surface sorbent materials [31]. In general, anion adsorption is strongly dependent on the pH of the medium, exhibiting the greatest removal in acidic to neutral solution. As has been demonstrated in previous studies, optimal Cr (VI) adsorption occurs at a pH lower than 4 for various sorbents, such as some metallic (oxy)hydroxides [32–34] and natural bio-sorbents, for example, larch bark [35], cooked tea dust [36], papaya seeds [37], raw Bagasse [38], and activated carbon [39]. In the case where iron and aluminum oxides are used as adsorbents, an adsorption efficiency of higher than 80% was reached at a pH of 4 to 6. The adsorption was seen to be highly dependent on the pH of the medium; the Cr (VI) uptake increased by increasing the pH values from 1.0 to 7.0, after which the uptake decreased.

Similar results were reported for the variation of hexavalent chromium adsorption with pH solution, with other adsorbents such as clay minerals [40], oxide-coated sand [40], aluminosilicate [41], zeolite [42], chitosan [43], and hydroxyapatite [44], which all exhibited a maximum uptake at a pH of 5 to 7. It has been suggested that, at a low pH, the adsorption is also low, due to the competition between the metal ions and protons for the adsorption sites. In these cases, the uptake of Cr (VI) followed the ion exchange mechanism. From these results, it could be concluded that, at a pH higher than pH_{max}, Cr (VI) exhibited typical anionic sorption behavior, with adsorption decreasing when the pH was increased. Similar results were reported for the retention of similar anions on oxide surfaces [45,46]. This adsorption pattern is the result of the protonation of surface hydroxyl sites and of Cr (VI) hydrolysis [47]. Thus, at a pH higher than pH_{max}, the retention of Cr (VI) was due to the interaction of $HCrO_4^-$ and/or CrO_4^{2-} with OH surface groups, rather than with OH_2^+ groups, which were predominant at a pH lower than pH_{max} [44]. The significant influence on the adsorption of CrO_4^{2-} was found at the slope of the pH adsorption edges. Distinct pH regions with different slopes characterized the various adsorbed species. This result reflected the change in the sorption mechanism [48].

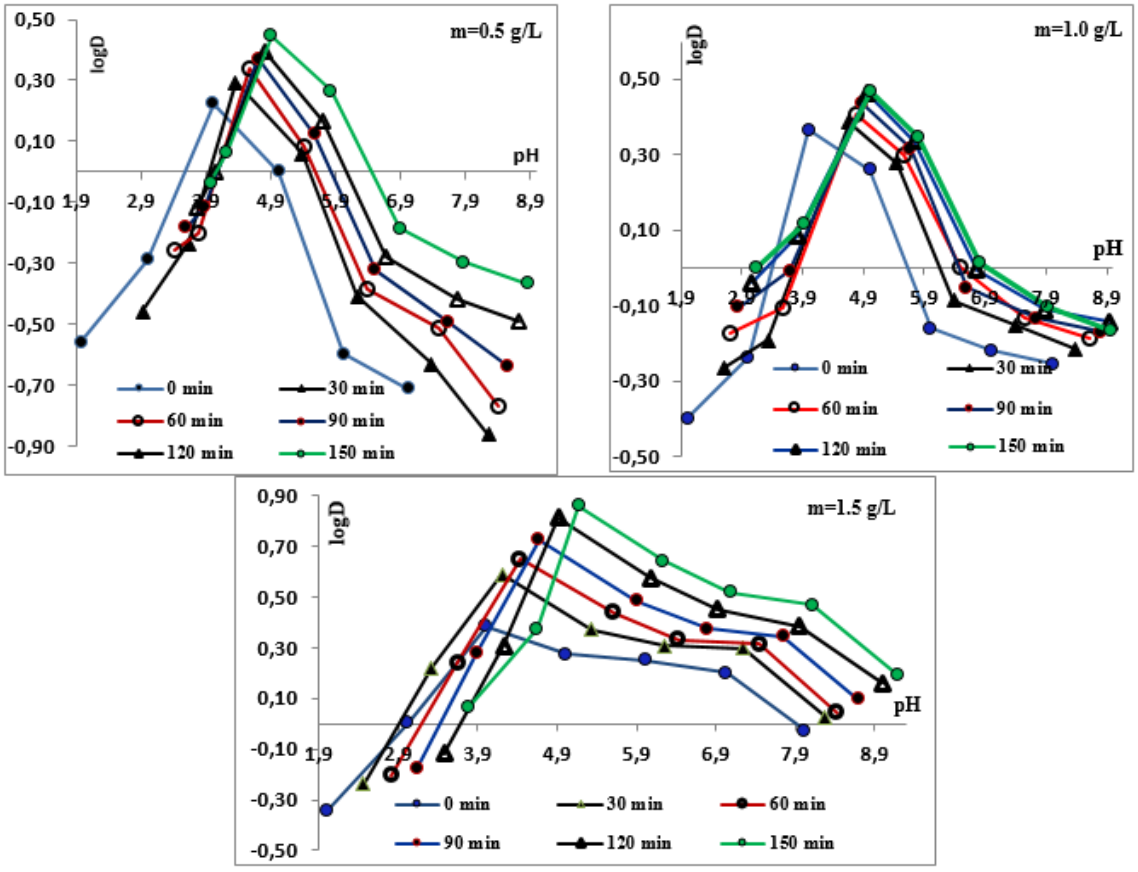

Figure 1. Log(D) versus pH for different amounts of OCP and different contact times.

3.2. *Effect of Contact Time*

The effect of contact time on the adsorption efficiency was examined, and the results are shown in Figure 2. At a pH lower than pH_{max}, a distinct difference was observed for adsorption envelopes in relation to the sorbent dose, or sorbet/sorbent ratio (surface coverage). At a sorbent dose of 0.5 and 1.0 g/L, the pH adsorption edges followed a similar trend for $t \geq 15$ min. At a pH of 50% of adsorption (pH_{50}), a negligible variation occurred at pH 3.9–4.1. When the sorbent dose was1.5 g/L, the adsorption process was dependent on the hydration time. Therefore, the adsorption envelopes

shifted to higher pH values, resulting in an increase in pH_{50} from 2.9 to 3.9, as the time increased from 0 to 150 min. The mechanism for the oxyanion adsorption was dependent on the surface coverage and hydration of the surface sites, involving the formation of distinct surface complexes. This was in agreement with the spectroscopic study results, which indicated that chromium (VI) resulted in the formation of both monodentate and bidentate surface complexes on iron oxides [49,50]. The proportion of these species was dependent on the metallic ion concentration. Recently, through the use of a spectroscopic study, it has been shown that the monodentate chromate complexes on ferrihydrite were predominant at a low surface coverage and a pH $\geq$ 6.5. In contrast, bidentate surface complexes were formed at a high surface coverage and pH $\leq$ 6 [51].

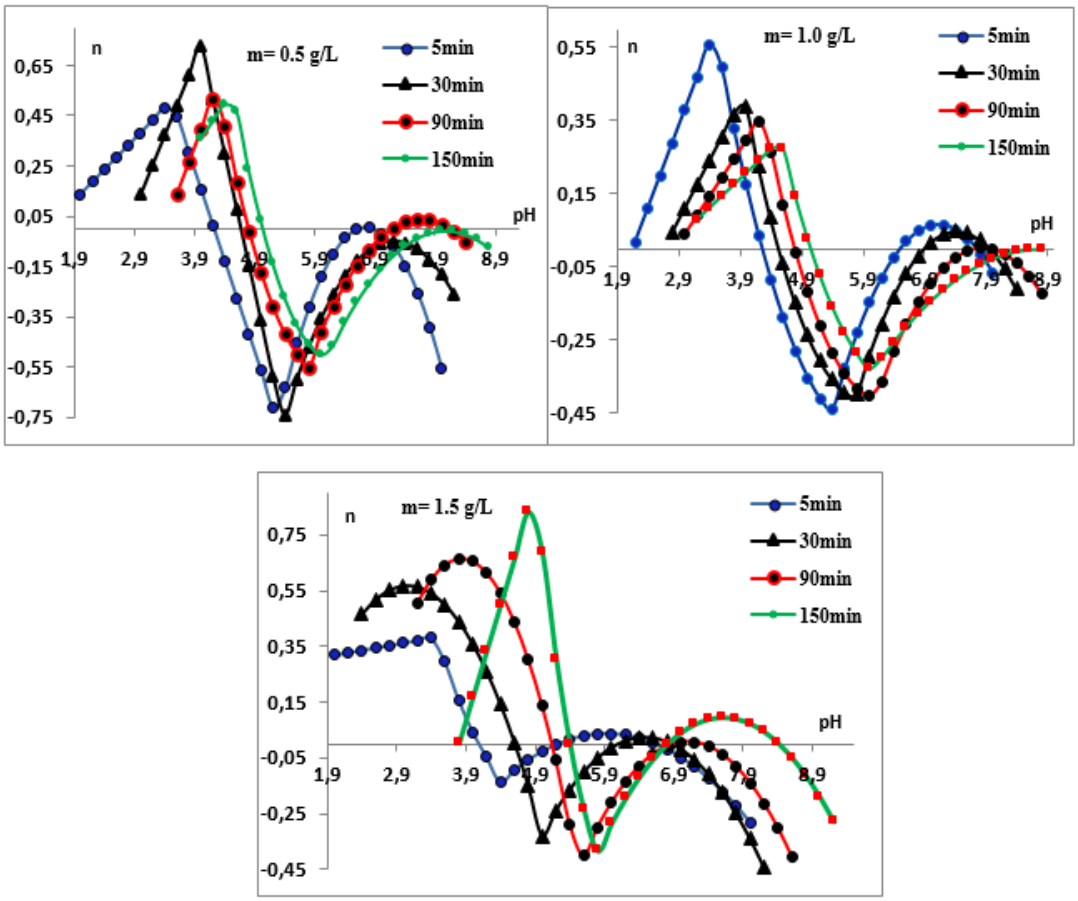

Figure 2. Variation of n = f(pH) obtained at various contact time and at different OCP sorbent amounts of m = 0.5, 1.0 and 1.5 g/L: 5 min (●); 30 min (▲); 90 min (●); and 150 min (■).

Taking into account the previous results, it could be deduced that, at a low adsorbent dose, monodentate surface complexes prevailed for all of the examined experimental conditions. In contrast, at a higher adsorbent dose, the bidentate surface complexes became predominant at a low hydration level of sorbent materials at pH $\leq$ pH_{max}, and were subsequently converted to monodentate species, when hydration equilibrium was reached.

At a pH higher than pH_{max}, adsorption envelopes become more alkaline. The shift to this alkalinity increased by increasing the hydration time. Due to electrostatic repulsion with the negative surface charges, the chromium uptake initially involved the adsorption of a $HCrO_4^-$ anion, which was followed by the subsequent slower, and less important, uptake of CrO_4^{2-} in the alkaline region. These electrostatic factors could influence both the kinetics and equilibrium of chromate ions, as observed for the adsorption of a similar oxyanion on ferrihydrite [52]. When the contact time increased, the adsorption of the chromate anion also increased, and the Log(D) = f(pH) curves show a

pronounced difference in the slopes at t = 150 min. As previously discussed, this phenomenon could be due to a change in the adsorbed fraction of the Cr (VI)-predominant surface complexes.

3.3. Chromium (VI) Adsorption Reactions and Stability Constants

The acid-based properties of calcium phosphate were described by the protonation and deprotonation reactions of the phosphate surface functional groups, as shown in Equations (1) and (2), $\overline{>SOH}$ [53,54]:

$$\overline{>SOH} + H^+ \leftrightarrow \overline{>S(OH_2)^+} \quad K^+ \tag{1}$$

$$\overline{>SOH} \quad \overline{\leftrightarrow > SO^-} + H^+ \quad K^- \tag{2}$$

K^+ and K^- were the surface stability constants, and the on lined species referred to the solid phase.

The adsorption reaction of chromium (VI) on calcium phosphate can be expressed as follows:

$$(>\overline{SOH)_l(H_iCrO_4)H_{-n}} + nH^+; \quad l = 1;2, \quad i = 1;2 \tag{3}$$

where n is the number of protons, which ranges from −1 to +1.

The initial ionization of H_2CrO_4 is relatively strong, so $HCrO^-{}_4$ was the main species found at pH > 5, and i = 1 at equilibrium (Equation (3)), under these conditions.

The symbol $H_{-n,}$ stands for both hydrogen atoms (n < 0) and for OH groups (n > 0). Taking into account that $H_2O \equiv H_{-1} + H_l$, the surface complexes $\overline{>(SOH)_l(H_iCrO_4)H_{-n}}$ noted thereafter $C_{ln,}$ represented a general formulation of species, differentiated by water composition. So $\overline{>(SOH)_l(H_2CrO_4)H_{-n}}$ could be $\overline{>(SOH)_l(HCrO_4)H_{-n+1}}$ + H_2O or $\overline{>(SOH)_l(CrO_4)H_{2-n}}$ + $2H_2O$, and even $\overline{>(S)_l(H_2CrO_4)H_{-n-l}}$ or $>(S)_l(HCrO_4)H_{-n-l+1}$ + H_2O or $>(S)_l(H_2CrO_4)H_{-n-l+2}$ + $2H_2O$.

The surface complexation constant for the relationship (3) is:

$$K_{ln} = \frac{\left[\overline{(>SOH)_l(H_iCrO_4)H_{-n}}\right][H^+]^n}{\left[\overline{>SOH}\right]^l\left[H_iCrO_4{}^{(i-2)+}\right]} \tag{4}$$

The distribution coefficient being:

$$D = \frac{\left[\overline{(>SOH)_l(H_iCrO_4)H_{-n}}\right]}{\left[H_iCrO_4{}^{(i-2)+}\right]} \tag{5}$$

where $[H_iCrO_4{}^{(i-2)+}]$ represents the equilibrium concentration of Cr (VI) in solution, it was obtained that:

$$\log D = \log K_{ln} + \log m + npH \tag{6}$$

where $\overline{>SOH}$ = m, was the concentration of sorbent used in g/L.

Assuming that the first approximation is the essential formation of mononuclear (l = 1), the surface complexes of Equation (6) become:

$$\log D = \log K_{1n} + \log m + npH \tag{7}$$

The variation of the distribution coefficient with pH allowed us to define the nature of the C_{1n}-adsorbed species. The values of (l,n) were obtained according to:

$$\left(\frac{\delta \log D}{\delta pH}\right)_m = n \tag{8}$$

So, the surface complexes of Cr (VI) with calcium phosphate could be well described from the experimental data logD = f(pH), shown in Figure 1. The analysis of the obtained results showed that the plots of logD = f(pH) were linear at various pH ranges. The straight lines of the slope correspond to the mean values of n, and varied between −1 and 1. The value of the surface complexes (1,n), involved in this case were (l,0), (l,1), (l,2), and (l,−1). In this case, the co-precipitation/adsorption process of chromium (VI), and the species distribution diagram as a function of pH, are needed. It is worth noting that the interaction of Cr (VI) with the OCP surface could be described as an n = f(pH) variation. For this purpose, fitting of the data into a polynomial equation was carried out for the three pH regions. The obtained results show that, when in acidic solution (pH < 5), a second-degree equation fitted (R^2 > 99%) the ascendant curve, whereas in low acidic to alkaline media, a cubic polynomial fitted (R^2 > 99%) two distinct segments of the descendant curve, at pH regions of about 4 to 6 and 6 to 10.

3.3.1. Surface Complexes and Effect of pH and Contact Time on H_3O^+/OH^- Exchange

The variations of n = f(pH) are illustrated in Figure 2. As shown in Figure 2, the protonation/deprotonating reaction followed a similar trend, with respect to the pH value. In all cases, the maximum H_3O^+ and OH^- exchange of $|n| = 0.8$ occurred at a pH range of 4.0–6.0. When considering the obtained results, it becomes evident that the H_3O^+/OH^- stoichiometry was not an integer, as might be expected from the theoretical single reaction. Similar results were observed for other adsorbed elements on iron (oxy) hydroxides [55,56].

It was assumed that the chromium adsorption occurred by different reactions, and consequently, resulted in a combination of at least two predominant surface complexes. In the case l = 1, the predominant complexes would be different for the sorbent amounts of 0.5 and 1.0 g/L, while a different adsorption behavior was observed for 1.50 g/L. Indeed, a low value of around 0.5 was found at low pH and at t < 150 min, indicating that C_{10} is not the predominant species under these conditions.

Taking into account these considerations, the uptake of Cr (VI), characterized by n = 0.5, and the general adsorption reaction, can be expressed by:

$$\overline{>SOH} + 2H_2CrO_4 \leftrightarrow \overline{>S(OH_2)^+(HCrO_4)_2H^{-n}} + 1H^+; \quad l = 1 \quad n = 2 \tag{9}$$

$$\overline{>SOH} + 2H_2CrO_4 \leftrightarrow \overline{>SH(HCrO_4)_2H^{-n}} + H_2O + nH^+; \quad l = 1 \quad n = 2 \tag{10}$$

The adsorption constant $K_{10.5}$ for equilibrium (10) was given by:

$$K'_{1n} = \frac{\left[\overline{>SH(HCrO_4)_2H^{-n}}\right]\left[H^+\right]^n}{\left[\overline{>SOH}\right]\left[H_2CrO_4\right]^2} = \frac{D \quad \left[H^+\right]^n}{\left[\overline{>SOH}\right]\left[H_2CrO_4\right]} \tag{11}$$

Based on this adsorption mechanism, the following relationship could be obtained:

$$\log(D(D+1)) = \log K'_{1n} + \log m + \log[Cr]_0 + n\,pH \tag{12}$$

For $[Cr]_0 = 10^{-4}$ M, which was the chromium analytical concentration used, the equation becomes:

$$\log(D(D+1)) = \log K'_{1n} + \log m - 4 + n\,pH \tag{13}$$

At a pH range of 2.5 to 5.0, the relation log(D(D + 1)) = f(pH) exhibited a linear variation, with slopes increasing from 0.5 to 1.0, as the time increased from 0 to 150 min.

Accordingly, C_{11}, $C_{10.5}$ and C_{10} were the predominant surface species in the case of l = 1. A non-protonated C_{11} ($\overline{>SOH(H_2CrO_4)H_{-1}} \equiv \overline{>S(HCrO_4)H_{-1}} \equiv \overline{>SCrO_4}$) complex was always formed at low acidity (pH ~4.4), combined with the protonated C_{10} ($\overline{>SOH(H_2CrO_4)H_0} \equiv \overline{>S(HCrO_4)H_0} \equiv \overline{>SHCrO_4}$), complex during hydration equilibrium conditions. Nevertheless, when this equilibrium was not reached at the 1.5 g/L sorbent amount, the C_{10} complex was

not favored, and disappeared, to the benefit of the bidentate: $C_{10.5}$ ($\overline{> SOH(H_2CrO_4)_2H_{-1}} \equiv \overline{> SH(HCrO_4)_2H_{-1}} \equiv \overline{> S(HCrO_4)_2}$) species. As a result, in this condition, $C_{10.5}$ and C_{11} were the prevailing complexes. The $C_{10.5}$ surface complex can also be formulated as the $\overline{> S(H_2Cr_2O_7)}$ species. However, the bichromate surface complexes were not found at 0.5 and 1.0 g/L sorbent doses and were neglected, as previously reported [57].

The results show that, as the sorbent amount increased, the number of surface sites also increased. At high-hydration equilibrium, the hydrogen chromate anions ($HCrO_4^-$) and water molecules were competing for the active surface sites. At a low-hydration level of the sorbent material's surface site, the $HCrO_4^-$ ions displaced the H_2O molecules, in the hydration sphere of the C_{11} complex. Bidentate surface species were then formed at a high sorbent dose and short contact time. These results were in accordance with previous studies, suggesting that high-chemisorbed water molecules prevented the bidentate complexes from forming, as noted for the complexation of chromium with ferrihydrite [48]. A similar substitution of water molecules by $HCrO_4^-$ anions could take place at a higher chromium concentration, even at hydration equilibrium, explaining the formation of bidentate surface species when there is a high surface coverage, observed for the adsorption of Cr (VI) or a similar anion on ferrihydrite [29].

It should be noted that the $C_{10} \equiv \overline{> S(HCrO_4)H_0}$ complex could also be expressed as an outer-sphere $\overline{> SOH_2^+ - HCrO_4^-}$ species, since we could not distinguish between the different complexes' formulations or structures, based on one H_2O molecule. Generally, when at a low pH value, the formation of such outer-sphere Cr (VI) surface complexes is favored, similar to that previously obtained on amorphous aluminum oxides [58], and supported by the formation of SOH_2^+ in acidic media, as was indicated in a titration experiment [59].

At a pH higher than 4.5, n varied between -1 and 0, in all investigated conditions. The predominant surface species formed in these conditions, were C_{10} and $C_{1\text{-}1}$. Thus, Cr (VI) was adsorbed via the formation of $\overline{> S(OH)(HCrO_4)H_0}$ (C_{10}) and $\overline{> S(OH)(HCrO_4)H_1}$ ($C_{1\text{-}1}$) complexes, that could be expressed as $\overline{> SCrO_4}$ and $\overline{> SHCrO_4}$, respectively. As the contact time increased, the optimal pH formation of protonated $C_{1\text{-}1} \equiv \overline{> SHCrO_4} \equiv \overline{> S(OH_2^+)(HCrO_4^-)}$ and the un-protonated $C_{10} \equiv \overline{> SCrO_4} \equiv \overline{> S(OH)(HCrO_4)}$ species, shifted from 5 to 6 and 7 to 8, respectively. The adsorption of Cr (VI) increased with t, and at a higher hydration time, the adsorption reaction was likely to comply to OH^- surface exchange. Thus, for a pH lower than PZC, the negative surface charge of the phosphate material reacts in acidic media to form $>S(OH_2)^+$, which adsorbs chromium as $HCrO_4^-$. Maximal OH^- exchange was observed at a pH range of 5.2–6.0, which approximately coincided with the pH range of zero charge and the iso-electric points of unloaded material. Whilst higher than PZC, the repulsion between chromium anions and negatively sorbent surface charge, increased with pH. The contribution of the columbic effect to the overall uptake of Cr (VI) could be a more important process. Nevertheless, at a pH value around the iso-electric point, the electrostatic repulsion reached a minimum value, and then the intrinsic process (with n = 0) became the major adsorption mechanism. As shown from the obtained results, the pH value became higher with contact time, reaching 8.2 at $t \approx 150$ min.

Consequently, the overall adsorption equilibrium could be obtained by the intrinsic reaction with 1 mole of H^+ (n = -1), or 1 mole of OH^- (n = 1) exchange reactions per mole of $HCrO_4^-$.

3.3.2. Equilibrium Constants

In the Log(D)= f(pH),Figure 1 plots the various contact times and sorbent amounts, and the straight lines show slopes ranging from -0.4 to 0.6. In the cases when the surface complexes are mononuclear (l = 1), apparent equilibrium constants, $K_{ap} = K_{1n}$ or K'_{1n}, were obtained from the origin ordinates $A = LogK_{1n} + Log(m)$ or $logK'_{1n} + Log(m) - 4$. From the obtained results, it can be that the variations of $logK_{1n} = f(n)$ (Figure 3) and $logK'_{1n} = f(n)$ (not shown), were linear under all experimental conditions.

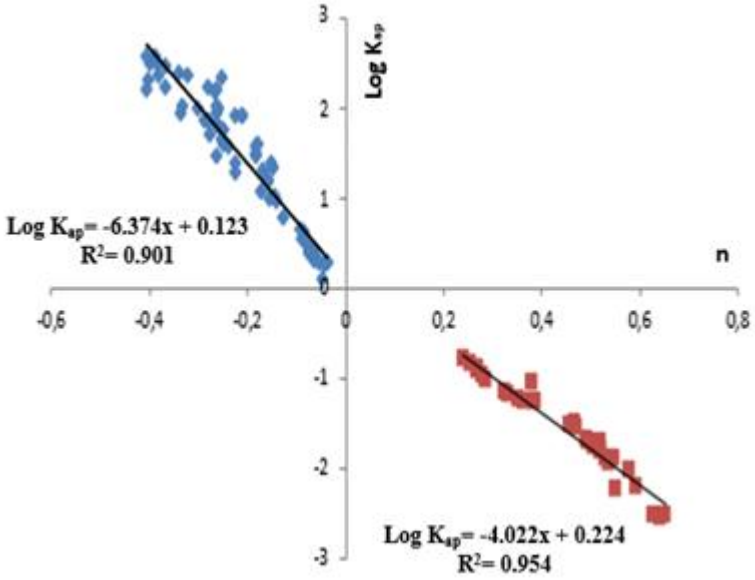

Figure 3. Variations of log Kap = f(n).

Taking into account that | n | also represented the fraction (x) of the predominant $1H^+$ or $1OH^-$ exchange reactions contributing to the overall adsorption equilibrium, the apparent constants (K_{ap}) of the overall equilibrium were given by the expressions shown in Equations (14) and (15):

$$K_{ap} = (K_{10})^{(1-|n|)} (K_{1\pm1})^{|n|} \quad (14)$$

$$\log K_{ap} = (1 - |n|)\log K_{10} + |n| \log K_{1\pm1} \quad (15)$$

with $K_{1\pm1} = K_{11}$ or K_{1-1}.

As an example, the overall partition equilibrium prevailing for pH > 5.5, and involving successive exchange reactions $n = 0$ and -1, can be summarized in the following reactions:

$$(1-x)(\overline{>SOH} + HCrO_4^- \leftrightarrow \overline{>S(OH)(HCrO_4)H_0} \equiv \overline{>S(CrO_4)} + H_2O): \quad (K_{10})^{(1-x)},\ n = 0 \quad (16)$$

Overall adsorption reactions are:

$$(x)(\overline{>SOH} + HCrO_4^- + H_2O \leftrightarrow (\overline{>SOH(HCrO_4)H_1} \equiv \overline{>S(HCrO_4)} + H_2O) + OH^-: \quad (K_{1-1})^x,\ n = -1 \quad (17)$$

$$\overline{>SOH} + HCrO_4^- + nH_2O \leftrightarrow (\overline{>SOH(HCrO_4)H_n} \equiv \overline{>S(HCrO_4)} + H_2O) + nOH^-: \quad (K_{1n}),\ -1 \le n \le 0 \quad (18)$$

Where x is the molar fraction of the sorption mechanism with 1 OH^- exchange. The apparent constant, $K_{ap} = K_{1n}$, is then given by:

$$\log K_{1n} = (1 - x)\log K_{10} + x \log K_{11} = (1 - |n|)\log K_{10} + |n| \log K_{10} \quad (19)$$

As shown above, the K_{ap} value could be determined experimentally, and was variable, depending on the surface charge and pH. Therefore, the constants K_{10} and $K_{1\pm1}$ were the intersect and the slope of $\log K_{ap} = f(n)$, respectively, whereas $K_{1\text{-}1}$ was the opposite of the slope. From this information, the intrinsic constants K_{10}, for H^+ (formation of $\overline{>S(OH_2^+)(HCrO_4^-)}H_0 \equiv \overline{>S(HCrO_4)}$) and OH^- (formation of $\overline{>S(OH)(HCrO_4)H_0} \equiv \overline{>S(CrO_4)}$) adsorption reaction exchange, were determined, with corresponding logarithmic values of $\log K_{10}$ = 0.2 and 0.1, respectively. The intrinsic constants ($K_{int} = K_{10}$) were obtained in general, by extrapolating the apparent constants to a zero surface charge [57,58].

As discussed previously, the variations of $\log K_{ap}$= f(n) could be due to the contribution of the electrostatic effect (K_{col}), related to K_{ap} [60,61] according to:

$$K_{int} = K_{ap}K_{col} = K_{ap}\exp(-nF\Psi_0/RT) \quad (20)$$

$$K_{ap} = K_{int}\,(K_{col})^{-1} = (K_{10})^{(1-|n|)}\,(K_{1\pm1})^{|n|} \quad (21)$$

In the particular case of $|n| = 1$, Equation (22) was obtained:

$$K_{ap} = K_{int}(K_{col})^{-1} = K_{1\pm1} \quad (22)$$

where ψ_0 was the surface potential, and R, T, and F were the gas constant, absolute temperature, and Faraday constant, respectively.

Since $K_{int} = K_{10}$, the columbic effect was determined according to

$$\log K_{col} = \log K_{10} - \log K_{1\pm1} \quad (23)$$

While $\log K'_{ap}$ for equilibrium (10) was:

$$\log K_{col} = \log K'_{10} - \log K_{10.5} \quad (24)$$

The origin ordinate of the $\log K'_{ln} = f(n)$ plots resulted in $\log K'_{10} = 5.3$. These results are summarized in Table 1.

Table 1. Surface complexation constants for Cr (VI) sorption onto Octacalcium phosphate.

Species	*n*	Adsorption Reaction	$\log K_{1n}$	$\log K_{col}$
		Acidic medium (pH < 5)		
$\overline{>SOH_2^+ - HCrO_4^-}$	0	$(\overline{>SOH}) + H_2CrO_4 \leftrightarrow \overline{>SOH_2^+ - HCrO_4^-}$	0.1	
$\overline{>SHCrO_4}$	0	$(\overline{>SOH}) + H_2CrO_4 \leftrightarrow \overline{>SHCrO_4} + H_2O$	0.1	
$\overline{>SCrO_4}$	+1	$(\overline{>SOH}) + H_2CrO_4 \leftrightarrow \overline{>SCrO_4} + H_2O + 1H^+$	−4.0	4.1
$\overline{>S(HCrO_4)_2}$	0.5	$(\overline{>SOH}) + 2H_2CrO_4 \leftrightarrow \overline{>SH(SCrO_4)_2H^-} + H_2O + 1H^+$	3.0	2.4
		Lower acidic to alkaline medium (pH > 5)		
$\overline{>SHCrO_4^-}$	0	$(\overline{>SOH}) + HCrO_4^- \leftrightarrow \overline{>SCrO_4^-} + H_2O$	0.2	
$\overline{>SHCrO_4}$	−1	$(\overline{>SOH}) + HCrO_4^- \leftrightarrow \overline{>SHCrO_4 + 1OH^-}$	−6.7	6.1

It is worth noting that the interaction of chromate anions with phosphate materials was of an essentially electrostatic nature in acidic media (pH < 5), and of a chemical character at a lower acidity (pH > 5) to alkaline solution. Two surface species were always formed when hydration equilibrium was reached; deprotonated ($\overline{>SCrO_4}$) and protonated ($\overline{>SHCrO_4}$) complexes, which were more stable in near neutral, than acidic, solution. This was consistent with modeling adsorption data, indicating a mixture of both monodentate and bidentate chromate surface complexes on goethite [62,63].

4. Conclusions

The adsorption of hexavalent chromium on OCP material was thoroughly investigated. One goal of this study was to develop a method for studying the surface complexation of OCP. The obtained distribution coefficient (D) was dependent on the contact time, pH, and surface coverage. The treatment of Log(D) = f(pH) experimental data were used to evaluate H^+/OH^- exchange stoichiometry in adsorption reactions, and the results were used to specify the predominant Cr (VI) surface species. At hydration equilibrium, protonated hexavalent chromium formed $\overline{>SHCrO_4}$ and unprotonated $\overline{>SCrO_4}$ complexes, under all explored conditions. When the hydration equilibrium was not reached at a low surface coverage, the protonated species disappeared, to the benefit of the bidentate ($\overline{>S(HCrO_4)_2}$) complex. The stability constants were $\log K_{10}$ = 0.123, for $\overline{>SHCrO_4}$, which could be formulated as $\overline{>S(OH_2^+)(HCrO_4^-)}$ and $\log K_{11}$ = −4.0 for $\overline{>SCrO_4}$, in acidic media.

In alkaline media, the log $K_{1\text{-}0}$ = 0.2 for $\overline{>SCrO_4)}$ and log $K_{1\text{-}1}$ = −6.4 for $\overline{>SHCrO_4}$. Whilst, for the bidentate $\overline{>S(HCrO_4)_2}$ surface species, the log$K_{10.5}$ = 2.9.The electrostatic effect was evaluated for the predominant adsorption reactions. The obtained results suggested that Cr (VI) adsorption on OCP was of an electrostatic nature in acidic solutions, and of a chemical nature in lower acidic to alkaline solutions. The results could have practical and promising applications in the fields of environmental health, for the removal of hazardous chromium from industrial wastewater before dumping it into the environment (water and soil). This could enhance the environmental risk management process and will play a major role in preventing future coastal contamination.

Abbreviations

OCP	Octacalcium Phosphate ($Ca_8H_2(PO_4)_{6.5}H_2O$)
XRD	X-ray Diffraction
FTIR	Fourier transform infrared spectroscopy
D	distribution coefficient (the ratio of concentration of adsorbed Cr (VI) to its concentration in aqueous phase)
m	OCP sorbent amounts in g/L
t	contact time.
K^+, K	surface stability of active site > SOH
l	number of functional surface group involved in adsorption reaction
H n	hydrogen atoms (n < 0) or OH groups (n > 0)
K_{ln}	adsorption constant
Ψ_0	surface potential
R	universal gas constant (8.31 J/mol·K)
T	temperature (K)

References

1. Dhal, B.; Thatoi, H.N.; Das, N.N.; Pandey, B.D. Chemical and microbial remediation of hexavalent chromium from contaminated soil and mining/metallurgical solid waste: A review. *Hazard J. Mater.* **2013**, *250–251*, 272–291. [CrossRef] [PubMed]
2. Zachara, J.M.; Ainsworth, C.; Brown, G.E., Jr.; Catalano, J.G.; McKinley, J.P.; Qafoku, O.; Smith, S.C.; Szecsody, J.E.; Traina, S.J.; Warner, J.A. Chromium speciation and mobility in a high level nuclear waste vadose zone plume. *Geochim. Cosmochim. Acta* **2004**, *68*, 13–30. [CrossRef]
3. Zhou, X.; Korenaga, T.; Takahashi, T.; Moriwake, T.; Shinoda, S. A process monitoring/controlling system for the treatment of wastewater containing Chromium (VI). *Water Res.* **1993**, *27*, 1049–1054. [CrossRef]
4. Tiravanti, G.; Petruzzelli, D.; Passino, R. Pretreatment of Industrial Wastewaters II, Selected Proceedings of the Second IAWQ International Conference on Pretreatment of Industrial Wastewaters. *Water Sci. Technol.* **1997**, *36*, 197–207. [CrossRef]
5. Pagilla, K.R.; Canter, L.W. Biosorption of Hexavalent Chromium from Aqueous Medium with Opuntia BiomassAthens, Greece. *Environ. J. Eng.* **1999**, *125*, 243–248. [CrossRef]
6. Bruce Manning, A.; Goldberg, S. Modeling Competitive Adsorption of Arsenate with Phosphate and Molybdate on Oxide Minerals. *Soil. Sci. Soc. Am. J.* **1996**, *60*, 121–131. [CrossRef]
7. Kongsricharoern, N.; Polprasert, C. Removal of Heavy Metals from Wastewater by Adsorption and Membrane Processes: A Comparative Study. *Water Sci. Technol.* **1996**, *34*, 109–116. [CrossRef]
8. Hu, J.; Chen, G.; Lo, I.M.C. Removal and recovery of Cr (VI) from wastewater by maghemite nanoparticles. *Water Res.* **2005**, *39*, 4528–4536. [CrossRef] [PubMed]
9. Dahbi, S.; Azzi, M.; de la Guardia, M. Removal of hexavalent chromium from wastewaters by bone charcoal. *Fresenius J. Anal. Chem.* **1999**, *363*, 404–407. [CrossRef]
10. Dahbi, S.; Azzi, M.; Saib, N.; de la Guardia, M.; Faure, R.; Durand, R. Removal of trivalent chromium from tannery waste waters using bone charcoal. *Anal. Bioanal. Chem.* **2002**, *374*, 540–546. [PubMed]
11. Hyder, A.H.M.G.; Shamim, A.B.; Nosa, O.E. Adsorption isotherm and kinetic studies of hexavalent chromium removal from aqueous solution onto bone char. *J. Environ. Chem. Eng.* **2015**, *3*, 1329–1336. [CrossRef]
12. Yoon, J. Phosohate-Induced Lead Immobilization in Contaminated Soil. Master's Thesis, University of Florida, Gainesville, FL, USA, May 2005.

13. Chowdhury, S.R.; Ernest Yanful, K. Arsenic and chromium removal by mixed magnetite-maghemite nanoparticles and the effect of phosphate on removal. *J. Environ. Manag.* **2010**, *91*, 2238–2247. [CrossRef] [PubMed]
14. Lee, J.Y.; Elzinga, E.J.; Reeder, R. Lead and zinc removal with storage period in porous asphalt pavement. *J. Environ. J. Sci. Technol.* **2005**, *39*, 4042–4048. [CrossRef]
15. Qureshi, M.; Varshney, K.G. *Inorganic Ion Exchangers*; Chemical Analysis CRC Press: Boca Raton, FL, USA, 2002; p. 282.
16. Correa, F.G.; Martínez, J.B.; Gómez, J.S. Synthesis and characterization of calcium phosphate and its relation to Cr (VI) adsorption properties. *Rev. Int. Contam. Ambient.* **2010**, *26*, 129–134.
17. Conca, J.L.; Lu, N.; Parker, G.; Moore, B.; Adams, A.; Wright, J.V.; Heller, P. Remediation of Chlorinated and Recalcitrant Compounds. *J. Environ. Qual.* **2000**, *7*, 319–326.
18. Saxena, S.; D'Souza, S.F. Heavy metal pollution abatement using rock phosphate mineral. *Environ. Int.* **2006**, *32*, 199–202. [CrossRef] [PubMed]
19. Aklil, A.; Mouflih, M.; Sebti, S. Removal of Cadmium from Water Using Natural Phosphate as Adsorbent. *Hazard J. Mater. A* **2004**, *112*, 183–190. [CrossRef] [PubMed]
20. Corami, A.; D'Acapito, F.; Mignardia, S.; Ferrini, V. Removal of Cu from Aqueous Solutions by Synthetic Hydroxyapatite: EXAFS Investigation. *Mater. Sci. Eng. B* **2008**, *149*, 209–213. [CrossRef]
21. Zhao, X.-Y.; Zhu, Y.-J.; Zhao, J.; Lu, B.-Q.; Chen, F.; Qi, C.; Wu, J. Hydroxyapatite nanosheet-assembled microspheres: Hemoglobin-templated synthesis and adsorption for heavy metal ions. *J. Colloid Interface Sci.* **2014**, *416*, 11–18. [CrossRef] [PubMed]
22. Serrano-Gómez, J.; Ramírez-Sandoval, J.; Bonifacio-Martínez, J.; Granados-Correa, F.; Badillo-Almaraz, V.E. Uptake of CrO42-Ions by Fe-Treated Tri-Calcium Phosphate. *J. Mex. Chem. Soc.* **2010**, *54*, 34–39.
23. Razzouki, B.; El Hajjaji, S.; ElYahyaoui, A.; Lamhamdi, A.; Jaafar, A.; Azzaoui, K.; Boussaoud, A.; Zarrouk, A. Kinetic investigation on arsenic (III) adsorption onto iron hydroxide (III). *Pharm. Lett.* **2015**, *7*, 53–59.
24. Soundarrajan, M.; Gomathi, T.; Sudha, P.N. Understanding the Adsorption Efficiency of Chitosan Coated Carbon on Heavy Metal Removal. *Int. J. Sci. Res. Publ.* **2013**, *3*, 2250–3153.
25. Sakai, S.; Anada, T.; Tsuchiya, K.; Ymazaki, H.; Margouli, H.C.; Suzuki, O. Comparative study on the resorbability and dissolution behavior of octacalcium phosphate, β-tricalcium phosphate, and hydroxyapatite under physiological conditions. *Dent. Mater. J.* **2016**, *35*, 216–224. [CrossRef] [PubMed]
26. Osamu, S. Octacalcium phosphate (OCP)-based bone substitute materials. *Jpn. Dent. Sci. Rev.* **2013**, *49*, 58–71.
27. Samake, D. Treatment of Tannery Wastewater Using Clay Materials. Ph.D. Thesis, Joseph Fourier-Grenoble University, Bamako, Mali, December 2008.
28. Zachara, J.M.; Cowan, C.E.; Schmidt, R.L.; Ainsworth, C.C. Chromate Adsorption by Kaolinite. *Clays Clay Miner.* **1988**, *36*, 317–326. [CrossRef]
29. Grossl, V.; Eick, M.; Sparks, D.; Goldberg, S.; Ainsworth, C.C. Arsenate and Chromate Retention Mechanisms on Goethite. 2. Kinetic Evaluation Using a Pressure-Jump Relaxation Technique. *Environ. Sci. Technol.* **1997**, *31*, 321–326. [CrossRef]
30. Lorphensri, O.; Intravijit, J.; Sabatini, D.A.; Kibbey, T.C.G.; Osathaphan, K.; Saiwan, C. Characterization of Commercial Ceramic Adsorbents and its Application on Naphthenic Acids Removal of Petroleum Distillates. *Water Res.* **2006**, *40*, 1481–1491. [CrossRef] [PubMed]
31. Harding, I.S.; Rashid, N.; Hing, K.A. urface charge and the effect of excess calcium ions on the hydroxyapatite surface. *Biomaterials* **2005**, *26*, 6818–6826. [CrossRef] [PubMed]
32. Zachara, J.M.; Girvin, D.C.; Scmidt, R.L.; Resch, C.T. Chromate adsorption on amorphous iron oxyhydroxide in presence of major ground water ion. *Environ. Sci. Technol.* **1987**, *21*, 589–594. [CrossRef] [PubMed]
33. Demetriou, A.; Pashalidis, I. Spectophotometric studies on the competitive adsorption of boric acid (B(iii)) and chromate (Cr(Vi)) onto iron (oxy) hydroxide (Fe(O)OH). *Glob. Nest J.* **2012**, *14*, 32–39.
34. Hsia, T.H.; Lo, S.L.; Lin, C.F.; Lee, D.Y. Chemica and spectroscopie evidence for specifie adsorption of chromate on hydrous iron oxide. *Chemosphere* **1993**, *26*, 1897–1904. [CrossRef]
35. Aoyama, M.; Tsuda, M. Removal of Cr(VI) from aqueous solutions by larch bark. *Wood Sci. Technol.* **2001**, *35*, 425–434. [CrossRef]

36. Odeh, L.; Odeh, I.; Khamis, M.; Khatib, M.; Qurie, M.; Shakhsher, Z.; Qutob, M. Hexavalent Chromium Removal and Reduction to Cr (III) by Polystyrene Tris(2-aminoethyl)amine. *Sci. Res. Acad. Publ.* **2016**, *6*, 26–37. [CrossRef]
37. Chang, L. Metal Ions Removal from polluted Waters by Sorption onto Exhausted Coffee Waste. Application to Metal Finishing Industries Wastewater Treatment. Ph.D. Thesis, University of Girona, Girona, Spain, September 2014.
38. Stankiewicz, A.I.; Moulijn, J.A. Process Intensification: Transforming Chemical Engineering. *Chem. Eng. Prog.* **2000**, *96*, 22–34. [CrossRef]
39. Oldham, D.J.; Mohsen, E.A. A technique for predicting the performance of self-protecting buildings with respect to traffic noise. *Noise Control Eng. J.* **1980**, *15*, 11–19. [CrossRef]
40. Bhattacharjee, S.; Swain, S.K.; Sengupta, D.K.; Singh, B.P. Effect of heat treatment of hydroxyapatite on its dispersibility in aqueous medium. *J. Colloids Surf.* **2006**, *277*, 164–170. [CrossRef]
41. Wu, X.W.; Ma, H.W.; Zhang, Y.R. Adsorption of chromium (VI) from aqueous solution by a mesoporous aluminosilicate synthesized from microcline. *Appl. Clay Sci.* **2010**, *48*, 538–541. [CrossRef]
42. Pandey, P.K.; Sharma, S.K.; Sambi, S.S. Kinetics and equilibrium study of chromium adsorption on zeoliteNaX. *Int. J. Environ. Sci. Technol.* **2010**, *7*, 395–404. [CrossRef]
43. Schmuhl, R.; Krieg, H.M.; Keizer, K. Adsorption of Cu(II) and Cr(VI) ions by chitosan: Kinetics and equilibrium studies. *Water SA* **2001**, *27*, 1–8. [CrossRef]
44. Asgari, G.; Rahmani, A.R. Preparattion of an Adsorbent from Pumice Stone and Its Adsorption Potential for Removal of Toxic Recalcitrant Contaminants. *J. Res. Health Sci.* **2013**, *13*, 53–57. [PubMed]
45. Dzombak, D.A.; Morel, F.M.M. *Adsorption of Inorganic Contaminants in Ponded Effluents from Coal-Fired Power Plants*; Massachusetts Institute of Technology Cambridge: Cambridge, MA, USA, 1985.
46. Farley, K.J.; Dzombak, D.A.; Morel, F.M.M. Distinguishing Adsorption from Surface Precipitation. *J. Colloid Surf. Sci.* **1985**, *106*, 226–242. [CrossRef]
47. Correa, F.G.; Gómez, J.S.; Martínez, J.B. Synthesis and Characterization of Inorganic Materials to Be Used as Adsorbents of Toxic Metals and of Nuclear Interest. In *Contributions of the National Institute of Nuclear Research to the Advance of Science and Technology in Mexico. Commemorative Edition 2010*; Instituto Nacional de Investigaciones Nucleares: Ocoyoacac, Mexico, 2010; pp. 195–210.
48. Müller, A.; Duffek, A. Similar Adsorption Parameters for Trace Metals with Different Aquatic Particles. *J. Aquat. Geochem.* **2001**, *7*, 107–126. [CrossRef]
49. Fendorf, S.; Eick, M.J.; Grossl, P.; Sparks, D. Arsenate and Chromate Retention Mechanisms on Goethite. 1. Surface Structure. *Environ. Sci. Technol.* **1997**, *31*, 315–320. [CrossRef]
50. Waychunas, G.A.; Fuller, C.C.; Davis, J.A. Surface complexation and precipitate geometry for aqueous Zn (II) sorption on ferrihydrite. *Geochim. Cosmochim. Acta* **2002**, *66*, 1119–1137. [CrossRef]
51. Mario, V.; Maya, A.T.; James, O.L. Surface Complexation Modeling of Carbonate Effects on the Adsorption of Cr(VI), Pb(II), and U(VI) on Goethite. *Environ. Sci. Technol.* **2001**, *35*, 3849–3856.
52. Raven, K.P.; Jain, A.; Loeppert, R.H. rsenite and Arsenate Adsorption on Ferrihydrite: Kinetics, Equilibrium, and Adsorption Envelopes. *Environ. Sci. Technol.* **1998**, *32*, 344–349. [CrossRef]
53. Perrone, J.; Fourest, B.; Giffaut, E. Surface and Physicochemical Characterization of Phosphates Vivianite, $Fe_2(PO_4)_3$ and Hydroxyapatite, $Ca_5(PO_4)_3OH$. *J. Colloid Interface Sci.* **2002**, *249*, 441–452. [CrossRef] [PubMed]
54. Smičiklas, I.; Dimović, S.; Plećaš, I.; Mitrić, M. Adsorption and removal of strontium in aqueous solution by synthetic hydroxyapatite. *Water Res.* **2006**, *40*, 2267–2274. [CrossRef] [PubMed]
55. Antelo, J.; Fiol, S.; Gondar, D.; López, R.; Arce, F. Comparison of arsenate, chromate and molybdate binding on schwertmannite: Surface adsorption vs. anion-exchange. *J. Colloid Interface Sci.* **2012**, *386*, 338–343. [CrossRef] [PubMed]
56. Gunnarsson, M. *Surface Complexation at the Iron Oxide/Water Interface Experimental Investigations and Theoretical Developments*; Institution för kemi Göteborgs University: Göteborgs, Germany, 2002.
57. Jain, A.; Raven, K.P.; Loeppert, R.H. Understanding Arsenate Reaction Kinetics with Ferric Hydroxides. *Environ. Sci. Technol.* **1999**, *33*, 1179–1184. [CrossRef]
58. Álvarez-Ayusço, E.; García-Sánchez, A.; Querol, X. Adsorption of Heavy Metals from Aqueous Solutions on Synthetic Zeolite. *Hazard J. Mater.* **2007**, *142*, 191–198.

59. Ellouzi, K.; Elyahyaoui, A.; Bouhlassa, S. Octacalcium phosphate: Microwave-assisted hydrothermal synthesisand potentiometric determination of the Point of Zero Charge (PZC) and isoelectric point (IEP). *Pharm. Lett.* **2015**, *7*, 152–159.
60. Jin-Wook, K. *The Modeling of Arsenic Removal from Contaminated Water Using Coagulation and Sorption*; Texas A&M University: College Station, TX, USA, 2005.
61. Singh, S.P.N.; Mattigod, S.V. Modelling boron adsorption on kaolinite. *Clays Clay Miner.* **1992**, *40*, 192–205. [CrossRef]
62. Eick, M.J.; Peak, J.D.; Brady, W.D. The effect of oxyanions on the oxalatepromoted dissolution of goethite. *Soil. Sci. Soc. Am. J.* **1999**, *63*, 1133–1141. [CrossRef]
63. Tanuma, Y.; Anada, T.; Honda, Y.; Kawai, T.; Kamakura, S.; Echigo, S.; Suzuki, O. Granule Size–Dependent Bone Regenerative Capacity of Octacalcium Phosphate in Collagen Matrix. *Tissue Eng. A* **2011**, *18*, 546–557. [CrossRef] [PubMed]